Advanced lab-class for bachelor students in Physics

Experiment T14

Stern-Gerlach

February 2023

Requirements

- spin of electrons
- movement of atoms in magnetic fields

Aim of the experiment

- Record data to obtain the distribution of the particle flow density in the detection plane without magnetic field and with different magnetic field strengths
- Investigation of the position of the maximum of the particle flow density as a function of the magnetic field inhomogeneity
- Determination of the Bohr magneton μ_B

Contents

References

[1] Böhm, M.: Höhere Experimentalphysik, Bd 272

[2] Mayer-Kuckuk, T.: Atomphysik, Bo 137

[3] Bergmann, Schaefer: Lehrbuch der Experimentalphysik, Band 4, Teil 1, Bd 15

[4] Haken, H., Wolf, H. C.: Atom- und Quantenphysik, Bo 164

[5] T. Hebbeker: Vorlesungsskript zur Experimentalphysik IV, Kapitel 8

[6] Phywe, Instructions for „Stern-Gerlach experiment“ LEP 5.1.11-00

[7] Old instructions for „Stern-Gerlach experiment“ by RWTH

[8] Petertill, M.: wall chart „Operating of the Stern-Gerlach apparatus“ in the lab

1 Introduction

In 1922 Otto Stern and Walther Gerlach, working at the Max Planck Institute in Frankfurt first conceived and performed the experiment that now bears their names. In this experiment they passed ionized silver atoms through an evacuated system in which an inhomogeneous magnetic field was present. An inhomogenous magnetic field was necessary because, when one considers a classically spinning magnetic dipole, it will precess due to the torque from the magnetic field it is in. If the field is homogeneous, the forces acting on the dipole cancel and the particle passes through undefelected. However, if the field is inhomogeneous, there is a non-zero net force acting on the particle and it's trajectory is deflected.

Electrically neutral atoms are used as opposed to simpole charged particles, e.g. electrons, so that deflection path is minimized and external electric fields to cancel charge effects need not be incorporated. This allows magnetic and spin-dependent effects to dominate. Silver was initially used because it had the correct electron structure, [Kr]$4d^{10}5s^1$, and is relatively inert (for a non-gas atom).

This experiment successfully showed that the direction of the angular momentum of a (silver in this case) atom is quantized. This was the first confirmation of the Bohr-Sommerfeld theory of "old quantum theory" dealing primarily with space quantization. Since the only unfilled orbital has a single electron in the outermost s-shell, the overall spin state of the atom can be treated as that of a spin $\frac{1}{2}$ particle. This quantizarion allows for a direct measurement of the Bohr magneton μ_B.

Similar experiments were repeated by many other physicists particularly using hydrogen atoms. In our version of the experiment, potassium atoms, structure: [Ar]$4s^1$, are used as it's less expensive than silver, but still the proper electron configuration.

2 Theoretical background

This section detaiils the theoretical background andw physical concepts on which the Stern-Gerlach experiment is based. Some derivations of the material can be found in the appendix and are referred to within the text. Other derivations are keft as an exericse for the reader, and should be handed in with the final report. Much of the material is collected from the various sources in the bibiliography, particularly refs. [7] and [8].

2.1 Magnetic moment and force

As explained in the introduction, it is necessary to determine the effect of applying an inhomogeneous magnetic field to the atomic magnetic moment. In the case of potassium is induced by the spin of a single electron.

The force along the z-component of the magnetic moment's motion is given by

$$F_z = \mu_z \cdot \frac{\partial B}{\partial z} = -m_s g_s \cdot \mu_B \cdot \frac{\partial B}{\partial z} \tag{1}$$

where the z-axis is chosen as quantisation axis, m_s is the quantum spin value, g_s is the Lande factor (≈ 2.00232 for an electron), μ_z is the magnetic moment in the z-direction, and B is the strength of the magnetic field through which the magnetic moment is passing. The derivation is an exercise for the reader.

2.2 Two-wire field

To create an inhomogeneous magnetic field, the pole shoes (shown in Figure 1) are used. Becuause of how the pole shoes aere shaped, it creates a magnetic field similar to that which is created by two parallel wires separated by a distance $2a$ having current flowing in opposite directions to each other. As shown in Figure 1, a is the radius of the convex pole shoe. This two-wire field causes the potassium beam to split. In fact, with a proper adjustment of the potassium beam a field gradient, $\frac{\partial B}{\partial z}$, can be achieved

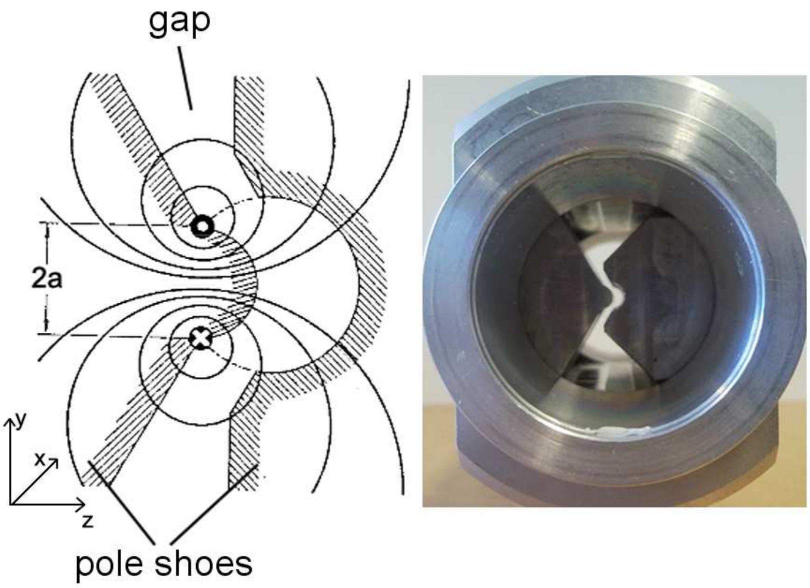

Figure 1: Pole shoes to produce a two-wire field

at a distance of about $\sqrt{2}a$ from the fictitious wires, which is approximately constant over the beam cross-section (see Appendix A.1). In practice, the field gradient can not be measured directly, but rather, is determined by measuring the magnetic induction B. For this, the following relationship can be used (derivation in Appendix A.1):

$$\frac{\partial B}{\partial z} = 0.9661 \cdot \frac{B}{a}. \tag{2}$$

The magnetic induction, B, is determined from the applied coil current by a calibration curve specific to each experimental set-up (Appendix B.1).
Exercise: Dervie the formula for a two-wire magnetic field starting from the Biot-Savart law.

2.3 Trajectory

The calcualtion of the Bohr magneton, μ_B, will require us to understand the trajectory that the potassium atom, with mass, m, takes through the setup. Because the particles are distributed randomly in the oven (with random velocity distribution), the trajectory are different. This is particularly important because the magnetic field gradient that the potassium atoms pass through is non-zero. Different particle trajectories are shown in Figure 2. We take the propagation direction of the particles to be in the x-direction, whereas the magnetic field acts along the z-axis. Here, the particle detected at position $u^{(2)}$ is faster than the one detected at $u^{(1)}$ ($\Delta u > \Delta z$). The particle observed at $u^{(3)}$ will have a different spin orientation with respect to the other two particles.

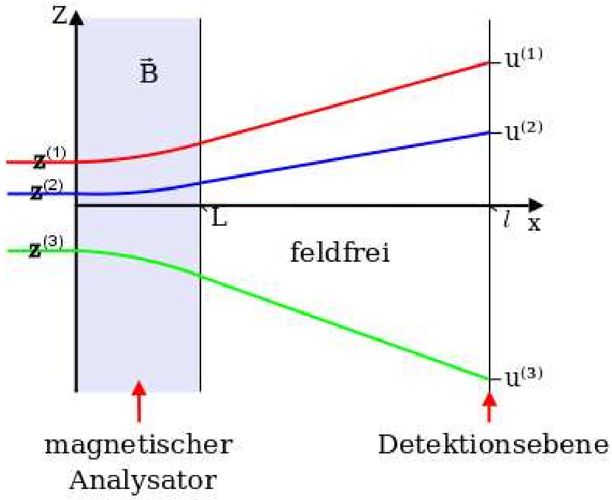

Figure 2: particle trajectories

The particles are acted on by a magnetic field over a length L, which takes the time $\Delta t = \frac{L}{v}$ through which to travel. The deflection, Δz, of the particle in z-direction is given by

$$\begin{aligned}\Delta z &= \tfrac{1}{2}\ddot{z}\,(\Delta t)^2 \\ &= \tfrac{1}{2}\cdot\tfrac{F_z}{m}\cdot(\Delta t)^2\,.\end{aligned}$$

Since $\Delta z \ll L$, it can be assumed that $\vec{v} \approx \vec{v_x}$. As the particle exits the magnetic field, its velocity, $\dot{z}$, in z-direction is given by the momentum $m\dot{z} = F_z \cdot \Delta t$. The potassium proceeds to move towards the detector at the position $x = l$, in a uniform and rectilinear way. The total time, t_{tot}, that the particle takes to reach the detector from the moment it enters the magnetic field is $t_{tot} = \frac{l}{v}$. It's now possible to calculate the impact point u of the particle as a function of its speed and the field inhomogeneity:

$$\begin{aligned}u &= z + \Delta z + \dot{z}\cdot(t_{tot} - \Delta t) \\ &= z + \frac{L\cdot l}{mv^2}\left(1 - \frac{L}{2l}\right)\mu_z\frac{\partial B}{\partial z} \\ &= z - \frac{L\cdot l}{mv^2}\left(1 - \frac{L}{2l}\right)m_s g_s\cdot\mu_B\frac{\partial B}{\partial z}.\end{aligned} \tag{3}$$

Faster particles are deflected less, because they spend a smaller amount of time inside the magnetic field.

2.4 Influence of the velocity distribution of the particles and the beam profile

As it was noted in the previous subsection, the velocity distribution has an effect on the distribution of the potassium atoms and the beam profile. A more formal description of the distribution and the spatial dependence of the particle flux at the detector is needed.

The potassium atoms form a gas when they are heated, and vaporized in the oven, which can be considered to be in thermal equilibrium at the operational temperature, T. Because of this, the potassium atoms satisfy the Maxwell velocity distribution everywhere in the oven, and the particle density, n, is identical everywhere inside the oven. Thus, the number of particles $\mathrm{d}N$ with a velocity between v and $v + \mathrm{d}v$ is

$$\mathrm{d}N \sim e^{-\frac{mv^2}{2kT}} v^2 \mathrm{d}v.$$

This thermal proportionality is also valid for the particles inside the potassium beam, leaving the oven. However, one still needs to take into account the geometrical proportionality that allows calculation of the beam profile, which has the following form for the uniform rectilinear propagation of the potassium atoms

$$\mathrm{d}N \sim v \, \mathrm{d}v.$$

Because of a system of collimating plates, only the potassium atoms moving (to good approximation) parallel to the beam direction leaving the furnace comprise the potassium beam. If one considers atoms with a given velocity, v, leave the oven in a sufficiently small time interval Δt, they may only originate from inside a volume of a length $v \cdot \Delta t$ in front of the slit (see figure 3). The size of this volume is directly proportional to the particle velocity, v. Since the particle density, n, is the same everywhere inside the entire oven, the number of atoms of a certain velocity, v, in the beam scales with v (in addition to the Maxwell velocity distribution).

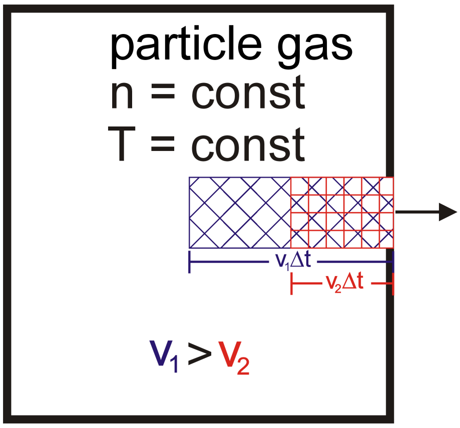

Figure 3: For the derivation of the geometric proportionality in the velocity distribution

As a result, one obtains

$$\mathrm{d}N \sim e^{-\frac{mv^2}{2kT}} v^3 \mathrm{d}v.$$

Since the quantity that is most useful is the number of particles as a function of the impact point, u, $\mathrm{d}v$ has to be substituted by $\mathrm{d}u$. Because the impact point for identical particles with the same speed and the same z only differs by m_s, according to the equation (3), one has

$$\begin{aligned} |u - z| &= \left| -\frac{L \cdot l}{mv^2} \left(1 - \frac{L}{2l}\right) m_s g_s \cdot \mu_B \frac{\partial B}{\partial z} \right| \\ &= \frac{L \cdot l}{mv^2} \left(1 - \frac{L}{2l}\right) |m_s| g_s \cdot \mu_B \frac{\partial B}{\partial z} \\ &= \frac{L \cdot l}{2mv^2} \left(1 - \frac{L}{2l}\right) g_s \cdot \mu_B \frac{\partial B}{\partial z}. \end{aligned} \tag{4}$$

In this experiment, the inhomogeneity of the magnetic field, $\frac{\partial B}{\partial z}$, is positive by definition. This leads to

$$v = \sqrt{\frac{L \cdot l}{2m} \left(1 - \frac{L}{2l}\right) g_s \cdot \mu_B \frac{\partial B}{\partial z} \frac{1}{|u - z|}}$$

and

$$
\begin{aligned}
\mathrm{d}v &= \sqrt{\frac{L\cdot l}{2m}\left(1-\frac{L}{2l}\right)g_s\cdot\mu_B\frac{\partial B}{\partial z}}\cdot\left(-\frac{1}{2}\right)|u-z|^{-\frac{3}{2}}\cdot\frac{u-z}{|u-z|}\mathrm{d}u \\
&= -\frac{1}{2}\sqrt{\frac{L\cdot l}{2m}\left(1-\frac{L}{2l}\right)g_s\cdot\mu_B\frac{\partial B}{\partial z}\frac{1}{|u-z|}}\cdot\frac{u-z}{|u-z|^2}\mathrm{d}u \\
&= -\frac{v}{2(u-z)}\mathrm{d}u. \qquad (5)
\end{aligned}
$$

Becuase only positive solutions are allowed for $\mathrm{d}v$, this results in

$$
\mathrm{d}v = \frac{v}{2|u-z|}\mathrm{d}u \qquad (6)
$$

as well as

$$
\begin{aligned}
v^3\mathrm{d}v &= \frac{v^4}{2|u-z|}\mathrm{d}u \\
&= \frac{1}{2}\left(\frac{L\cdot l}{2m}\left(1-\frac{L}{2l}\right)g_s\cdot\mu_B\frac{\partial B}{\partial z}\frac{1}{|u-z|}\right)^2\frac{1}{|u-z|}\mathrm{d}u \\
&= \frac{1}{8}\left(\frac{L\cdot l}{m}\left(1-\frac{L}{2l}\right)g_s\cdot\mu_B\frac{\partial B}{\partial z}\right)^2\frac{1}{|u-z|^3}\mathrm{d}u. \qquad (7)
\end{aligned}
$$

Therefore, taking into account the normalization, the total number of particles as a function of the impact point is:

$$
\mathrm{d}N = \frac{a\cdot e^{-\frac{b}{|u-z|}}}{|u-z|^3}\mathrm{d}u, \qquad (8)
$$

with

$$
\begin{aligned}
a &= \frac{\frac{1}{8}\left(\frac{L\cdot l}{m}\left(1-\frac{L}{2l}\right)g_s\mu_B\frac{\partial B}{\partial z}\right)^2}{2\int\limits_{-\infty}^{\infty}\frac{1}{8}\left(\frac{L\cdot l}{m}\left(1-\frac{L}{2l}\right)g_s\mu_B\frac{\partial B}{\partial z}\right)^2 e^{-\frac{b}{|u-z|}}\frac{1}{|u-z|^3}\mathrm{d}u} \\
&= \frac{1}{2\int\limits_{-\infty}^{\infty}e^{-\frac{b}{|u-z|}}\frac{1}{|u-z|^3}\mathrm{d}u} \qquad (9) \\
b &= \frac{L\cdot l}{4kT}\left(1-\frac{L}{2l}\right)g_s\cdot\mu_B\frac{\partial B}{\partial z}. \qquad (10)
\end{aligned}
$$

Here, the factor 2 in front of the integral is due to the fact that, because of symmetry considerations, both flight directions (into and out of the furnace) are equally likely.
The finite dimensions of the beam and the beam profile have the following additional proportionality:

$$
\mathrm{d}N \sim \Phi_m(z)\mathrm{d}z,
$$

$\Phi_m(z)$ describes the number of particles that travel between z and $z+\mathrm{d}z$ within the magnetic field, where the index $m=\pm\frac{1}{2}$ denotes the orientation of the magnetic moment. Thus, the final distribution function is

$$
\mathrm{d}^2N = \Phi_m(z)\frac{a\cdot e^{-\frac{b}{|u-z|}}}{|u-z|^3}\mathrm{d}u\mathrm{d}z \qquad (11)
$$

2.5 Ideal case, method A

It is now possible to specify the particle current density, $I(u)$, as a function of the impact point, u, on the detector. To consider all particles of the beam, one has to take an integral of z and sum over all possible spin orientations:

$$
\begin{aligned}
I(u) &= \frac{1}{\mathrm{d}u}\left(\sum_m \int_{-D}^{D} \mathrm{d}^2N\right) \\
&= \left(\sum_m \int_{-D}^{D} \frac{\mathrm{d}^2N}{\mathrm{d}u}\right) \\
&= \left(\sum_m \int_{-D}^{D} \Phi_m(z)\frac{a\cdot e^{-\frac{b}{|u-z|}}}{|u-z|^3}\mathrm{d}z\right). \qquad (12)
\end{aligned}
$$

Since the distribution of the number of particles in the beam is equivalent for both orientations, $m_s = \pm\frac{1}{2}$, the following definition can be made

$$\Phi_{+\frac{1}{2}}(z) \equiv \Phi_{-\frac{1}{2}}(z) := \frac{I_0(z)}{2}.$$

Therefore,

$$I(u) = a\int_{-D}^{D} I_0(z)e^{-\frac{b}{|u-z|}}\frac{\mathrm{d}z}{|u-z|^3}. \qquad (13)$$

Now, consider the approximation of an infinitesimal narrow box for the beam profile described by:

$$I_0(z) = 2DI_0\delta(z).$$

Here $\delta(z)$ is the Dirac delta function, for which (if x_0 is within the limits of integration) the following applies:

$$\int f(x)\delta(x-x_0)\mathrm{d}x = f(x_0).$$

This results in

$$I(u) = 2aDI_0e^{-\frac{b}{|u|}}\frac{1}{u^3}. \qquad (14)$$

From this, the maxima of the intensities can be determined. To do this, equation (14) is differentiated and set equal to zero:

$$
\begin{aligned}
\frac{\mathrm{d}I(u)}{\mathrm{d}u} &= 2aDI_0\frac{b-3|u|}{u^5}e^{-\frac{b}{|u|}} \stackrel{!}{=} 0, \\
\Rightarrow u_0^{(0)} &= \pm\frac{b}{3} = \pm\frac{L\cdot l\left(1-\frac{L}{2l}\right)}{12kT}g_s\cdot\mu_B\frac{\partial B}{\partial z}. \qquad (15)
\end{aligned}
$$

From inspection of eq.([?]), it is clear that the position of the maxima, u_0, increases linearly with the field inhomogeneity, i.e.

$$u_0^{(0)} = \text{const.}\cdot\frac{\partial B}{\partial z}. \qquad (16)$$

From here on, this method is referred to as method A.

2.6 Real beam cross-section, method B

2.6.1 Beam cross-section

The previous method assumes many ideal conditions and the real case can be better described by better approximation of the beam cross section geometry. Assuming a $2D$, finite width, beam cross section, the beam profile can be described by a parabolic central peak with the edges of the parabola being described by straight lines, as shown in Figure 4. This is described by the following piecewise description for the particle current density

$$I_0(z) = i_0 \cdot \begin{cases} D + z & \text{for } -D \leq z \leq -p \\ D - \frac{1}{2}p - \frac{1}{2}\frac{z^2}{p} & \text{for } -p \leq z \leq p \\ D - z & \text{for } p \leq z \leq D \end{cases}$$

This leads to the following 1st and 2nd derivatives with respect to z

$$\frac{\mathrm{d}I_0(z)}{\mathrm{d}z} = i_0 \cdot \begin{cases} 1 & \text{for } -D \leq z \leq -p \\ -\frac{z}{p} & \text{for } -p \leq z \leq p \\ -1 & \text{for } p \leq z \leq D \end{cases} \tag{17}$$

$$\frac{\mathrm{d}^2 I_0(z)}{\mathrm{d}z^2} = i_0 \cdot \begin{cases} 0 & \text{for } -D \leq z \leq -p \\ -\frac{1}{p} & \text{for } -p \leq z \leq p \\ 0 & \text{for } p \leq z \leq D \end{cases}$$

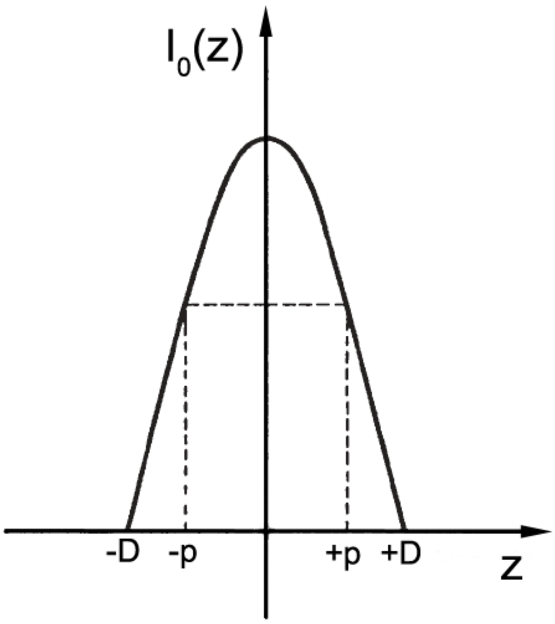

Figure 4: Mathematical approach for the particle current density in case of a vanishing magnetic field

In this case, p is defined as the value that z takes where the parabolic bahvior transitions to linear, and D is the z-intersection of this function.

2.6.2 Asymptotic behaviour for large fields

In the presence of sufficiently large magnetic fields, it is possible to derive an equation for u_0 by performing a Taylor expansion to the function desribing the real beam cross section (cf. Appendix A.2, setting equation (22) to 0).

$$0 = \left(D^2 - \frac{1}{3}p^2\right)\left(\frac{b}{u_0} - 3\right) + \frac{D^4 - \frac{1}{5}p^4}{u_0^2}\left(5\left(\frac{b}{u_0} - 1\right) + \frac{1}{12}\frac{b^2}{u_0^2}\left(\frac{b}{u_0} - 15\right)\right)$$

Here, the first term is the first-order solution in first order, while the second term represents a higher order correction term. If the higher order corrections are neglected, this leads to the solution $u_0^0 = \frac{b}{3}$. Since the second term is a higher order correction term, the substitution u_0 by u_0^0 can be used because the resulting variations will be of an even higher order. This yields the following approximation:

$$\begin{aligned}
0 &= \left(D^2 - \frac{1}{3}p^2\right)\left(\frac{b}{u_0} - 3\right) + \frac{D^4 - \frac{1}{5}p^4}{u_0^2} \\
\Rightarrow b &= 3u_0 - \frac{D^4 - \frac{1}{5}p^4}{D^2 - \frac{1}{3}p^2}\frac{1}{u_0} = 3u_0 - \frac{C}{u_0}. \qquad (18)
\end{aligned}$$

The correction term $-\frac{C}{u_0}$ takes into account the different amount of force applied at different positions in the beam cross section. In the analysis section, the Bohr magneton μ_B will also be calculated using both Method A and Method B (described in this section).

Exercise Use the equations (10) and (18) to find an expression, in which μ_B only depends on quantities measured in this experiment.

3 Operational and Safety Instructions

This section describes the phyical systems that comprise the experimental setup for the Stern-Gerlach apparatus. The various electronic circuits are described in some detail. Then some attention is given to the pumping system. The detection principle is then discussed followed by instructions for collecting the data.

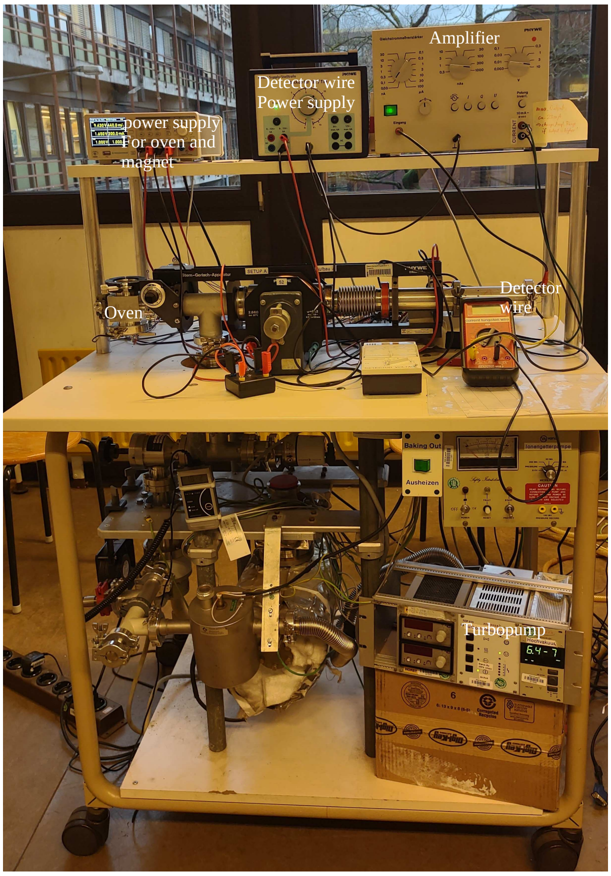

Figure 5: Stern-Gerlach apparatus in the lab course

> To prevent damage to the detector, it is essential to make sure that the **matching transformer** is connected between the voltage source and the **detector**.

For the operating voltages see table 1, the dimensions needed for the analysis can be obtained from table 2. Initially, the power source for the solenoid has to be turned off.

device	operation mode	setting
furnace	heating (ca. 20 min.)	800–900 mA$_{=}$
	continuous operation	ca. 420–480 mA$_{=}$
detector	normal operation	4.2 A$_{\sim}$
magnet		max 2.0 A$_{\sim}$

Table 1: settings

3.1 The electronic circuits

There are many different circuits that provide different functionality to the Stern-Gerlach apparatus.

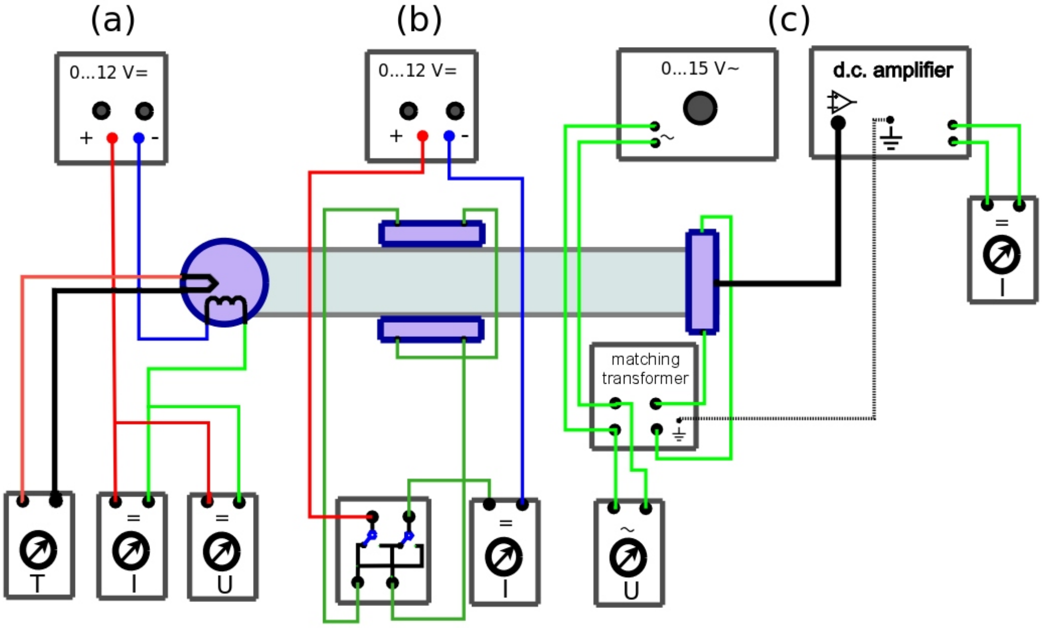

Figure 6: Electric circuit for: (a) furnace; (b) magnetic analyser; (c) detector. The meters represent ADC read-out points.

length of the pole shoes	$L = 7 \cdot 10^{-2}$ m
radius convex pole shoe	$a = 2.5 \cdot 10^{-3}$ m
from start of magnetic field to detector	$l = 0.455$ m

Table 2: dimensions of the apparatus

1. Oven/heating circuit
2. Thermocouple circuit
3. Magnetic field circuit
4. Particle detection circuit
5. Detector movement circuit
6. Readout circuit

3.1.1 The oven/heating circuit

Elemental potassium begins to evaporate when it reaches temperatures exceeding 60 $\circ$. Only reaching this temperature boils off a very tiny number of particles that, due to the laws of statitical mechanics and kinematics for gaseous particles, one would not expect to be able to detect any particles at the detector wire. Thus, a significantly higher temperature is required. The temperature range which is sufficient for detecting potassium atoms at the detector wire is an integral exercise of this experiment. As potassium is heated beyond its boiling point, an incresing amount of potassium is boiled of as the temperature of the oven is increased. It should be noted that potassium is expensive and running at a higher temperature than necessary tends to only serve to waste potassium that could be used in future running of the experiment. Therefore, under no circumstances should the oven be operated at a temperature higher than 180 $\circ$C.

Prior to performing detailed measurements, a coarse set of measurements should be made with the maximum magnetic field strength applied. These measurements should be made starting at a relatively low temperature, e.g. 100 $\circ$C, and repeated in steps of 5–10 $\circ$C. The purpose of this is to determine

at what temperature peak splitting is observed and determine at what temperature the setup should operate. The temperature should allow for the peaks to be sufficiently differentiated in space. It is critical for the analysis portion that the temperature remain constant throughout the remaining data collection of the experiment.
After the temperature has been stabilized, the magnetic field can be turned off. As you reduce the strength of the magnetic field, invert the field several times to help minimize magnetic hysteresis effects.
The heating is controlled by the oven/heating circuit. The circuit consists of a DC power supply connected in series with the oven and a 10 mΩ resistor. The current is controlled by the power supply and the passes through a resistive element attached to the oven. As current passes through the oven's circuit element, the element heats up and transfers heat to the oven, which is in thermal contact with the potassium and heats the potassium. The current then passes through the resistor and back into the power supply completing the circuit. This resistor serves asa measurment point for the micrcontoller to read the current (actually, it's voltage that has some math performed on it, but more on this when discussing the read-out circuit).

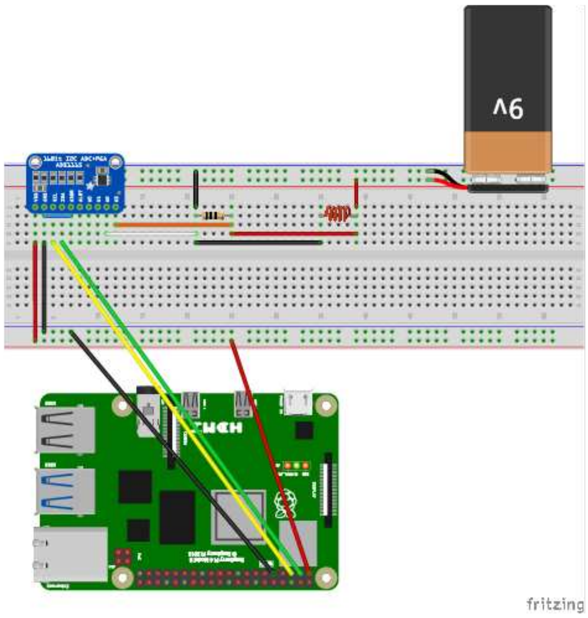

Figure 7: The oven current circuit for the Stern Gerlach setup. The DC power supply for the oven is represented here by a 9 V battery while the oven is represented by an inductor. These are connected in series with a 10 mΩ resistor. The oven current is measured by an ADC with analog inputs A_2 and A_3 connected across the resistor. The ADC is connected to the Raspberry Pi via I2C (SCL and SDA) connections and the 3.3 V and GND supply power to the ADC. The ADC ADDR pin is connected to GND to indicate that it's the top-level ADC.

3.1.2 The thermocouple circuit

As the oven is heating, a type-J thermocouple measures the current by producing a voltage difference $\mathcal{O}$(0-10 mV). The thermocouple has two Pamona jacks attached to to be used with a standard voltmeter. These jacks are connected across a 1 kΩ resistor. The voltage across this resistor is measured by the microcontroller and converted into a temperature value.

3.1.3 The magnetic field circuit

To generate the magnetic field, current is passed in seires through two separate magnet solenoid coils, one on each side of the setup. These solenoids are positioned such that the center of the coil field aligns well with the center of the magnetic pole shoes in the apparatus. The strength of the field is controlled by the current supplied by the power supply. This power supply is the same as that used to heat the

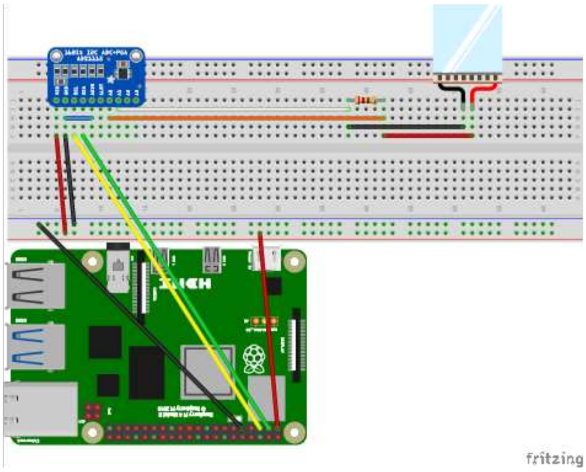

Figure 8: The temperature reading circuit for the Stern-Gerlach setup. This is only a simplified portion of the specific part of the circuit to show the functionality. The thermocouple directly measuring the temperature of the oven is connected across a 1000 Ω resistor. The resistor is connected across the analog inputs A_0 and A_1 of the ADC. The ADC is the top-level since it's ADDR pin is connected to GND. The I2C connections (SDA and SCL) and the 3.3 V and GND supply are connected to the Raspberry Pi GPIO pins.

oven, though a different channel is used. As the current through the solenoid increases, so does the magnetic field strength. However, this behavior is complicated and is detailed in the plot the Appendix. To determine the magentic field strength, simply note the current applied to the coils and read the associated point on the plot in the Appendix.
The current travels from the power supply through a switch connected in series with the two coils (in series with each other), and then through a 10 mΩ resistor. The switch simply changes the direction of the current and thus the direction of the magnetic field applied by the solenoid coils. The resistor functions as a means for the microcontroller to read the current (again here it's actually voltage) supplied by the power supply that passes through the coils so that it can be converted into a magnetic field value. It should be carefully noted that the current through the solenoid coils should never exceed 2.0 A. If one looks carefully at the associated plot for the magnetic field in the Appendix, it is clear that the magnetic field strength approaches an assymptote starting from about 1.0 A and no information is available much beyond 1.4 A. It is instructive to consider how many different values of the magnetic field is needed to get a 'complete' set of measurements to decide at which current values the setup should be operated at. Here again, a look at the plot in the Appendix can be helpful.

3.1.4 The particle detection circuit

The Stern-Gerlach experiment makes use of a Langmui-Taylor detector. This is a detector typically used to observe electrically neutral atoms. It consists of a tungsten wire that, when operated, is heated to 800 $\circ$C and is surrounded by a nickel cylinder with an entrance window for the potassium beam. A matching transformer is operated via an AC power supply that supplies $\approx$ 50 V to the wire. Without the bias voltage, the detector would provide a current, as it otherwise operates as an incandescent light bulb. This current would increase exponentially with the temperature of the wire.
The cylinder is grounded, thus when the potassium atoms hit the wire, they are ionized. For the potassium atoms, the ionization energy is lower than the work function for electrons in tungsten. The atoms are then accelerated by the electric field from the potrential difference generated by the wire and the cylinder. The resulting current is $\mathcal{O}$(pA) and needs to be amplified.
If the tungsten wire has the correct temperature, the measured current is proportional to the number of potassium atoms detected. If the detector current is too low, not all of the potassium atoms will be ionized. However, if the detector current is increased, a discharge current can be measured despite the bias voltage. This discharge current increases as the wire temperature increases.

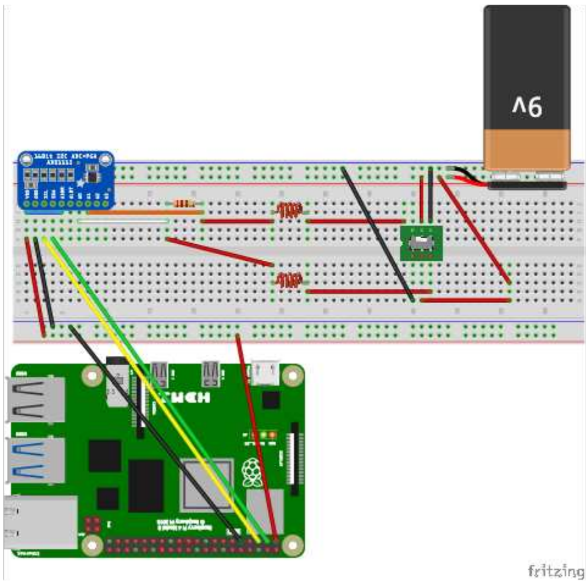

Figure 9: The circuit for reading the current generating the magnetic field responsible for splitting the potassium beam. The current is supplied by a DC power supply (represented here by a 9 V battery) connected to a double pull double throw switch connected in series with a pair of solenoids (represented here by inductors) and a 10 mΩ resistor. The ADC reads the voltage across the resistor similar to the previous circuits. The primary difference is that for this ADC, the ADDR pin is connected to the $V_D D$ pin making it a secondary ADC.

It is also immportant to note that contaminants (oxygen, nitrogen, water vapor, tungsten, etc.) on the wire, remaining from before the system is evacuated, can evaporate and contribute an erroneous signal as these atoms become ionized as well. A further item of importance is that the coaxial cable connecting the read-out of the wire to the amplifier is touched, this can cause errouneous signal since the current is extremely small and sensitive to such variations. So, contact with this cable should be avoided as much as possible. If contact is made with this cable simply wait 10-15 s for the current to stabilize before continuing.
The powering circuit for the wire is formed by the AC power supply on one side of the transformer and the detector wire on the opposite side. The signal circuit is formed by the read-out BNC coaxial cable connecting from the detector wire to the amplifier. The output from the amplifier passes through a 100 mA resistor which is read-out by the microcontroller circuit.

3.1.5 The detector movement circuit

The detector is controlled mechanically using a precision-graduated knob which is connected to a control arm that allows the detctor wire (in fact the entire portion of the setup down-beam of the magnet) to move left or right. The knob is graduated in units of 100 graduations per full rotation. The screw connecting the knob to the control arm is also attached to a NEMA-17 stepper motor. This stepper motor is driven by an L298N stepper motor driver board controlled by the microcontroller. This driver has a separate 5 V power circuit. You will control the stepper motor using a PYTHON program on the Raspberry Pi.

3.1.6 The read-out circuit

The above circuits are read-out and controlled using the Raspberry Pi microcontroller. For a full description of the Raspberry Pi microcontroller, please see the appropriate subsection later. We will focus on the necessary properties to understand the circuit and perform the measurements.
The microcontroller read-out circuit reads 5 different observables and controls the stepper motor. The five quantities measured by the microcontroller are:

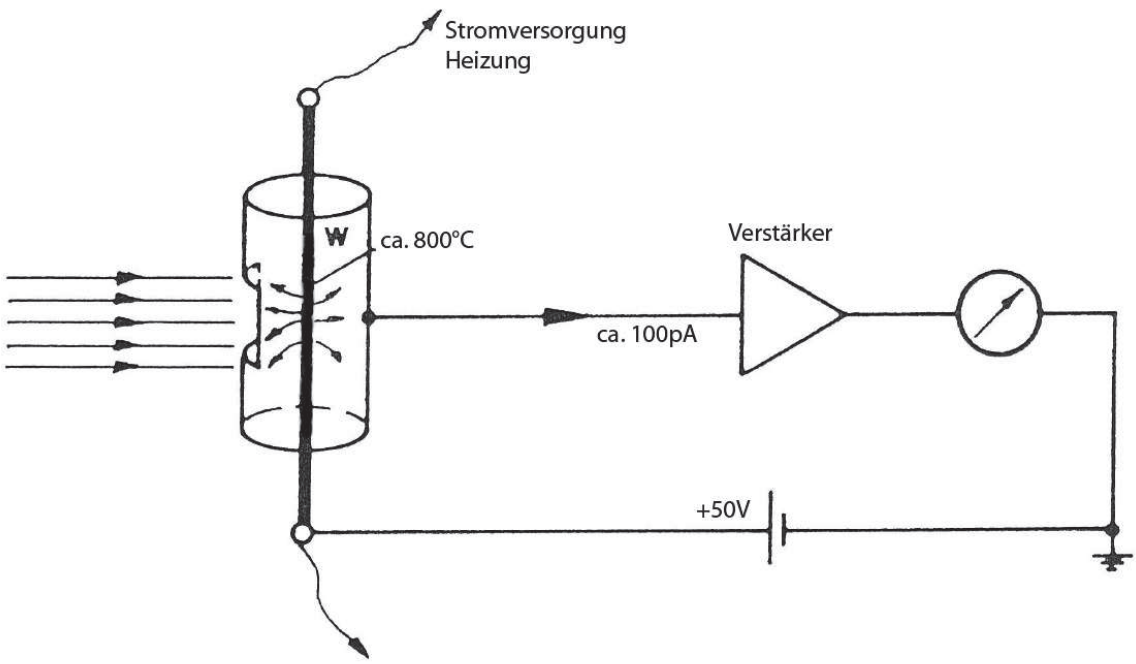

Figure 10: Sketch of the Langmuir-Taylor detector

- Oven temperature
- Oven current
- Magnetic field current
- Transformer supply voltage
- Detector wire signal current

The typical read-out circuit mimics a voltmeter connection. The full readout is actually a "schematic sum" of the five circuits, where we mean that each of the circuits above is a piece of the large circuit. The basic circuit design for the oven temperature, oven current, magnetic field current, and the signal current are the same.

Before we get to the actual circuit, we should describe the general ADC connections. The ADS1115 ADC board has connection pins. The power supply for the board connects to the $\mathrm{V}_D D$ connection and ground to the GND pin. The I2C intefaces through the SCL and SDA (serial clock and serial data, respectively) connections; these are how the data is actually transferred between the ADC and the Raspberry Pi. There is an address (ADDR) pin that is used by the PYTHON program and the Raspberry Pi to distinguish between each ADC when multiple ADCs are used within the same circuit, like in our case. The address is differentiated by connecting the ADDR pin to one of either the $\mathrm{V}_D D$, GND, SCL, or SDA pin. The particular address is not important unless you have to dig into the code if the circuit needs to be troubleshooted. In general, if you believe that there is a problem with the circuit, you should contact the experiment supervisor.

The other pins are comprised of an ALERT pin and four analog input pins A_0–A_3. The ALERT pin is not used here and we will ignore it for this experiment. The other analog input pins are generally connected across a read-out resistor. The general approach for the analog input connections is for A_0 and A_1 to be connected across one read-out resistor and A_2 and A_3 are connected across another read-out resistor. This is done to perform a differential read in which the ADC simply calculates the voltage difference in (ADC bits) between the two analog inputs (A_0–A_1 and A_2–A_3). Thus, since there are five measured quantities, there are two completely utilized ADCs and one that is partially utilized.

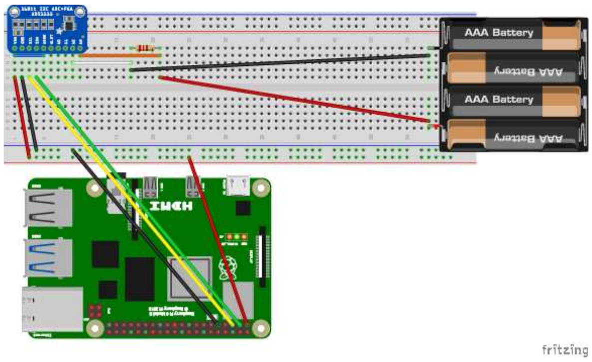

Figure 11: The signal current readout circuit consists of an amplifier (represented here by a block of AAA batteries) that translates the current measured by the Langmuir-Taylor detector into a current that can be measured by more traditional means connected to 500 mΩ resistor. The ADC is connected in a manner similar to the previous circuits with the exception that its ADDR pin is connected to the $\mathrm{V}_D D$ pin making it a secondary ADC.

3.2 Vacuum system

The entire experimental set-up is placed in a ultra-high vacuum system. Otherwise, the experiment would not be possible at atmospheric pressure due to the interaction of the potassium atoms with gas atoms in the air. Prior to starting the experiment, use the cold cathode vacuum gauge to confirm that the pressure is less than: $p \approx 4 \cdot 10^{-6}$ mbar. The reason for this specific requirement is that if the detector wire will quickly burn out and data collection will not be possible without replacing the detector wire. This process takes several days, so make sure to proceed carefully. When heating the furnace , the vacuum may get worse. The pressure might increase (up to 2 orders of magnitude is possible), however the system should recover within 5–10 minutes. If it does not recover after 15 minutes, please report it to the supervisor! **If the pressure rises above 10^{-4} mbar at any point of time, immediately turn off the detector and report to the supervisor.** If the detector is not turned off, it can burn out in a matter of minutes!

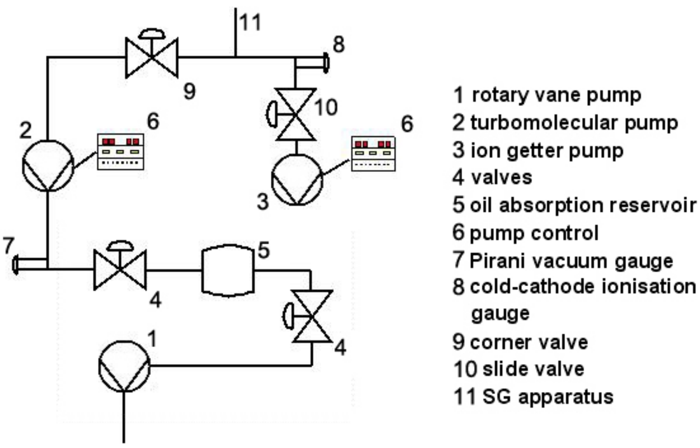

Figure 12: Schematic set-up of the vacuum pump system

3.3 The Raspberry Pi and the PYTHON programs

This iteration of the Stern-Gerlach experiment will use a Raspberry Pi as the master data acquisition and handler of the experiment. Experiment operation and control will be done by the web-based GUI via a tablet. The GUI will initiate the PYTHON programs found on the Raspberry Pi described below.

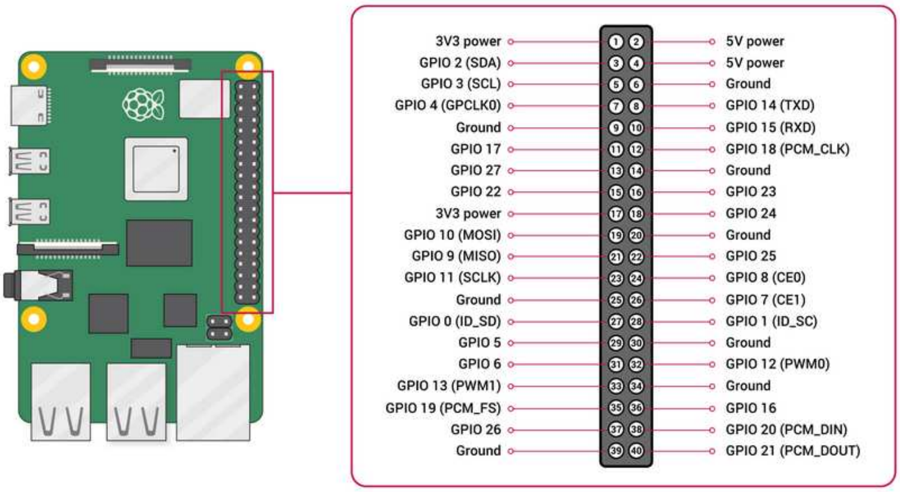

https://www.raspberrypi.org/documentation/computers/os.html

Figure 13: Pinout of the Raspberry Pi 4B showing each pin's functionality

However, if the GUI stops working for an unforeseen reason we outline the steps for operating the setup using only the Raspberry Pi. Two PYTHON programs already installed on the Raspberry Pi will be used to operate the apparatus and assist with data collection. The programs do not allow for full automation. The DC and AC power supplies as well as the amplifier need to be operated manually. Additionally, the detector supply current is read from a digital multimeter. We briefly describe the functionality of the Raspberry Pi and how the PYTHON programs are written and intended to be used.

3.3.1 The Raspberry Pi

The Raspberry Pi performs two functions in this lab experiment. Firstly, it serves as the PC with operating system which provide the student with the interface to acquire data. Secondly, it serves as the microcontroller interacting and acquiring the data. We will discuss these and any pertinent information for the student required to complete the experiment here.

For this experiment, we use the Raspberry Pi 4B as the data collection and storage medium. The Rasberry Pi is a single-board computer that has recently found popularity for teaching basic computer science principles as well as more niche applications such as robotics. There are several different models of the Rasberry Pi 4 available, the 4A, 4B, and 4Zero. The primary difference between the different models is the size and maximum available memory. We choose to use the 4B model as it optimizes size and available computing resources.

The RaspberryPi is similar to most other Linux-based PCs in that it has an operating system, CPU, RAM, and hard data storage. It comes equipped with a 1.5 GHz 64-bit quad core ARM Cortex-A72 processor. It does not come with a pre-built OS like most PCs that you could buy from a retailer, however its parent company provides two supported OSs. These are Raspbian and Raspebrry Pi OS. The two are very similar, though the primary difference is that Raspberry Pi OS is offered in a 64-bit version that can utilize the maximum RAM available on the PC, while Raspbian is a 32-bit architecture that utilizes a maximum of 3 GB of RAM. The only hardware resource that differentiates the types of 4B models is the amount of available RAM. Thus, the Raspberry Pi is available to be purchased with 1, 2, 4, and 8 GB of RAM.

The Raspberry Pi 4B has a fair number of peripherals that can be connected. It also has 4 USB A connections, 2 USB 2.0 and 2 USB 3.0. The 4B has two micro-HDMI connection supporting two monitors simultaneously. The Rasberry Pi has a USB C connection that allows appropriate AC/DC power supplies to be connected. It also has an RJ-45 gigabit ethernet connection to support wired internet. The Pi also comes with on-board Wifi and Bluetooth 5.0 capability.

The Raspberry Pi provided will contain the desktop version of Rasbian which is a debian-based LINUX operating system. If you are unfamiliar with operating a LINUX system, there are many great tutorials available online. However, we will only use simple commands on the Terminal. The Terminal is a program

very similar to that of the Command Prompt on Windows PCs. To open a terminal, simply click on the terminal icon and it should pop open a terminal prompt.
The commands that will be used are quite simple. We will cover the most common ones here. If you want to make a new directory named ‘data’, you would execute (excluding the quotes): ‘mkdir data’. The ‘cd’ command is used when you wish to change directories. For example, if you are in the home directory (in LINUX this is the ~/) and you want to change to the ‘data’ directory you would execute (again, without quotes): ‘cd data’. To copy a file, it has the form: ‘cp <path_to_file> <path_to_where_file_should_go>’. To read a file, the EMACS text editor is included. If you are familiar with a different editor (e.g. pico, nano, vim, etc.) you are welcome to use them if they are already included. To open a file with EMACS, use the command: ‘emacs -nw <name_of_file>’. If you are unfamiliar with how to use EMACS special key short cuts, brief explanations can be found online, or ask your lab supervisor. If we need any LINUX commands that are more complicated than this in any of the mini-experiments, we will explicitly describe them in the relevant sections.
As the Raspberry Pi serves as the primary PC, it has its own operating system, Raspbian. Raspbian is a debian-based LINUX distribution specifically for ARM devices. ARM stands for Advanced RISC Machine, and RISC stands for Reduced Instruction Set Computer architecture. The important aspect of ARM architecture is that it attempts to provide a framework for computers to simplify instructions given to them to accomplish a task. Advances in this architecture have allowed for the production of computers like the Raspberry Pi and similar to be built that are fast and powerful for only being the size of a large credit card. Of course it can’t compete directly with a state-of-the-art desktop PC, but it gives significant processing power to wireless applications in computing and robotics, etc.
The student will interact with the Raspberry Pi directly as if it is a desktop PC. To turn the Rasberry Pi on, simply plug the power supply into the electrical outlet. After sometime, the login screen will appear. The username is ’pi’ and the password will be supplied by the experiment supervisor. The student will only need to open a Temrinal window to begin working and this can be accessed by clicking on the Terminal windo icon found under the ’Accessories’ tab in the menu.
The directory structure is very simple. To start working from the Terminal the student can enter the command:

```
cd sternGerlach
```

There will be two PYTHON programs:

- testSG.py
- testStepper.py

These programs will be described in more detail in the next subsection.
We now turn our focus to the Raspberry Pi as a microcontroller. The Raspberry Pi has 40 GPIO pins. Each pin provides a dedicated function. These functions are noted on the Raspberry Pi 4B pinout. The Raspberry Pi utilizes the 3.3 V pin and GND pins to supply the driving current to all parts of the circuit. There are five sets of pins that can provide I2C functionality, however this setup only makes use of one pair (SCL and SDA). These pins provide the actual flow of serial data and clocking/timing information so that it can colate the incoming data properly. There are quite a few other pins that can serve as input or output pins. We only use these pins to control the stepper motor driver to move the detector wire.

3.3.2 The PYTHON programs

There are two PYTHON programs that the student will use to take data listed in the previous subsection. We will start by considering the testStepper.py program. The function of this program is straight-foward, to send a signal to rotate the control knob to move the detector wire. If the interested student looks into the code, they will notice that it is quite complicated because the code has to control the bipolarity of the stepper motor in a very careful way. **DO NOT MODIFY THE CODE UNLESS INSTRUCTED TO DO SO!!!**
The important information for the student is how to use this program to actually turn the knob with the stpper motor. The testStepper.py program takes four (4) arguments as input:

- -r This flag tells the program how many full rotations to apply

- -g This flag tells the program how many graduations (less than a full rotation) to apply in addition to the -r flag (less than 100)
- -d This flag controls the direction to turn the knob. The direction is 'l' or 'r' for left/right respectively as the direction that the knob is rotating when looking at the top of the knob. So, left is counter clockwise and right is clockwise.
- -c This flag tells the program if it should expect the motor to change directions from what it last moved. So, if it was moving clockwise and now needs to move clockwise this flag would be true and is implemented using '1' and if no change in direction is desired it's implemented with a '0'. This is important because this flag is used to account for the slack or play in the knob when changing direction. There is about a 10 graduation play when changing direction and this accounts for it.

It should be noted that to help prevent turning too many full rotations and damaging the motor if the setup can't move the detector wire (control arm only moves so far and then is stopped mechanically), and the motor still wants to turn, this would damage the motor, there is an internal program limit of -r 3 -g 80 (3 full rotations plus 80 graduations). An example of running the program would be simply typing:

```
python3 testStepper.py -r 2 -g 35 -d r -c 1
```

This would would tell the program to expect a change in direction (-c 1) to add 10 grads to the calculation, rotate in clockwise direction (-d r) for 2 full revolutions (-r 2) plus 35 graduations (-g 35). This program is mainly used to set the knob to the correct starting position. It should also be noted the knob can be moved slightly by hand (no more than 10 grads to avoid damaging the motor) if the position is off slightly.

The other program, testSG.py is the primary program that the student will use. This program will collect data from the ADCs that measure the different quantities that need to be recorded and/or displayed. This program will collect all of the data related to the setup as mentioned in "The read-out circuit" section. The program rotates the knob to move the detector wire by 2 grads waits 4 seconds for the setup to stabilize and reads the data from the ADCs and displays them on the screen. Each measurement is separated by a line of plus '+' signs. The knob reading and the signal current is recorded in an output text file. Each reading takes about 5 second in total.

To run the program do the following:

```
python3 testSG.py -o <outputFileName>
```

where <outputFileName> is the name of the output file that you would like to use. This program will step through a full range of detector positions once. It will stop itself automatically and then needs to be reset. So, this program needs to be run for each run at a specific magnetic field value that you want to perform.

3.4 Recording of the measurement series

For the following measurements, the furnace temperature has to be kept constant. The detector current in the detection plane should be measured without magnetic field and at different magnetic field strengths up to the one corresponding to a coil current of 1.2 A. The measurements should be performed in small steps, since an accurate determination of the position of the maxima with magnetic field turned on as well as the beam parameters p and D with $B = 0$ has to be performed. In order to keep magnetic remanence effects low, one should take care to carried out the measurements in a way that the coil current is only increased.

It is important to consider that the range of the d.c. amplifier has to be adjusted if necessary. The detector is moved 1.8 mm per turn.

For each run, confirm that the detector knob is set to the proper value (7.00). Run testSG.py and let it run (should end at 0.00). When it finishes, use testStepper.py to move the knob back to 7.00. Change the magnetic field if needed. Rerun testSG.py with a new output file name. Repeat until you have collected your data.

3.5 Changing the oven and magnetic field current

The current for the oven and magnetic will be changed using the GUI. However, in the event of an unforeseen problem, the student may be required to operate the power supply manually. We describe that here. To do this, do the following:

1. Select the channel using the top row of buttons (1a or 1b in the figure). Channel 1 (1a) controls the oven and channel 2 (1b) controls the magnetic field.

2. Using the left-most column of buttons (immediately next to the display) and select the current (I/2b) with the appropriate button.

3. Using the knob (3a), change the current to the desired value.

4. The arrow buttons (3b) adjacent to the knob can be used to move the digit (tens, hundreds, etc.) that is changed by the knob if necessary.

5. It may be necessary to also change the voltage (1a/b + 2a) if the current shows red and does not reach the expected value.

6. Only increase the voltage enough to reach the desired current, do not go higher.

7. To apply the current for, e.g. channel 1 (4a), press the "CH1 ON/OFF" button.

8. Then press the "MASTER ON/OFF" button (5) such that both buttons are illuminated after pressing.

If these buttons are not on, there will be no flow of current in the system.
Make sure to turn these buttons off when changing the current or voltage!!!

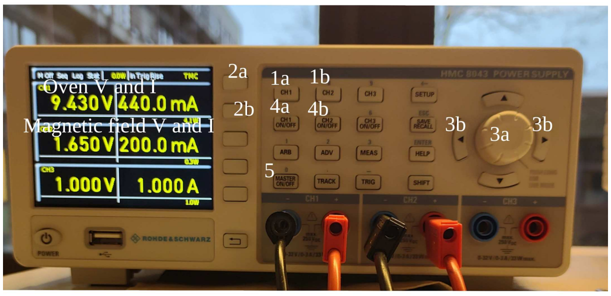

Figure 14: Picture of the LV supply to control the current through the oven and the magnetic field solenoids.

3.6 Experimental Readout

This section will describe the readout of the experiment. As described earlier in this instruction manual, the Raspberry Pi is running a program that collects information from various parts of the apparatus. This information can be monitored using a web-based GUI accessed using a browser on a tablet provided by the instructor. In addition to monitoring the state of the system and the data being collected, the GUI can control the power supply and the stepper motor. The last interesting part of the GUI is that some preliminary plots are shown "in real time" so that if there are problems they can be observed more quickly. We go into more detail on each of the GUI items here.

3.6.1 Monitoring the setup using the GUI

Fig. 15 shows the primary measurable quantities relative to the experiment that the Raspberry Pi includes. The left column shows the labels, the middles column is where the values go (here placeholder names are used), and the last column is the units. The quantities read by the Raspberry Pi and displayed in the GUI are:

1. The dial value showing the position of the detector wire. It is a unitless number or "subtick". This literally corresponds to the number read on the dial and the difference in subsequent subticks is 18 μm. This quantity is used as an axis to plot the signal current against.

2. The oven temperature is measured in units of degrees C.

3. The oven supply current (in mA) is measured directly as the output of the DC power supply. This should be modified as needed to either change the oven temperature or keep it constant.

4. The coil supply current (in mA) is also measured directly as the output of the DC power supply. This should be modified as needed in between data collection sets.

5. The signal output current (in mA) is measured as the oputput of the amplifier which amplifies the signal it receives from the tungesten detector wire. This is the key measurable in this experiment.

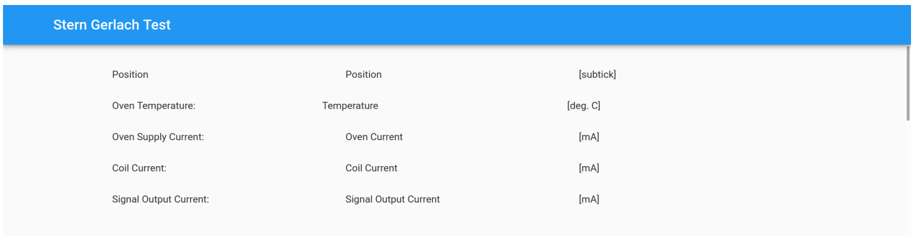

Figure 15: A screenshot of the GUI used to monitor and control the setup. The five primary measureable quantities are shown: detector wire position, oven temperature, oven supply current, coil supply current, and signal output current.

3.6.2 Controlling the Dial Position using the GUI

It's possible to control the stepper motor to turn the dial of the apparatus, thereby moving the detector wire to a different position. The primary options relating to this are shown in Fig. 16. We will briefly describe these here.

1. The "Dial Reset Movement Type" row contains a dropdown menu and a button. The dropdown menu has two options "List(Pos2-Pos1)" and "Number of Steps". It is strongly recommended to use the "Number of Steps" selection. The first option ideally takes the "Target Dial Position" entry and subtracts from the "Current Dial Position" entry to calculate how far to rotate the dial. Because of how the dial changes value e.g. 1,0,20,... it is easy to input the quantities in a way that causes the program to calculate the proper value correctly. Simply using the number of steps is safer remembering that there are 100 steps (subticks) per full rotation of the dial. The sign of the number matters for directional purposes. The "Number of Steps" option simply takes the value input into the "Number of Dial Steps to Move" entry as the value of interest. The "Set Dial Position" button then will move the dial based on the selected input from the dropdown (if the appropriate entries have been filled) once clicked.

2. The "Current Dial Position" row has a single entry where the current position of the dial can be input and used as "Pos1" in the "List(Pos2-Pos1)" option for moving the dial. Also used as the initial data value for starting a data run when clicking the "START DATA COLLECTION" button.

3. The “Target Dial Position” row has a single entry where the dial position that you would like to move to can be input and used as “Pos2” in the “List(Pos2-Pos1)” option for moving the dial. Also used as the final data value of a data collection when using the “START DATA COLLECTION” button.

4. The “Number of Dial Steps to Move” row has a single entry where the total number of steps that you would like to move the dial can be input. Remeber that there are 100 steps in a full rotation of the dial and that the sign of this number is used to control the direction.

5. The “Step Size [dial ticks]” row has a single entry where the number of dial ticks moved per step during a data collection can be set. Note that the recommended minimum number used here is 4, though it is possible to try with smaller values. Also because of the minimum angle that the stepper motor can move through, it is recommended to use even valued step sizes, e.g. 4, 6, 8, ..., 32, ... etc.

6. The “Target Temperature” row has an entry where a target temperature (deg. C) can be entered and a button to set this value. It is strongly recommended to NOT USE this setting. It is difficult to calculate how excatly the oven current should be automated as the required oven current to keep a constant temperature depends on a complicated set of variables. As such, this function is not guaranteed to keep the temperature constant under all circumstances.

7. The “STOP DATA COLLECTION” button controls the starting and stopping of collecting a data set. When clicking this button, it will interrupt and stop the data collection run and change the name of the “STOP DATA COLLECTION” button to “START DATA COLLECTION”. Which can be clicked to start the data collection process providing that the “Current Dial Position”, “Target Dial Position”, and “Step Size [dial ticks]” entry fields have been filled.

8. The “STOP TEMP ADJ” button will interrupt the temperature setting process initiated by the “SET TEMPERATURE” button.

9. The “CLEAR DATA” button will clear all data collected during the experiment. This needs to be done in between each data run for two reasons. First, the amount of storage in the database is not large and the data collected in a single run can be a significant fraction of the total storage space, therefore it is recommended to save it then delete it in betwen each run. Second, the data stored in the database is used to plot and visualize the data and after a few datasets have been collected the plot becomes very crowded.

10. The “STOP STEPPER” button will interrupt the movement of the stepper motor and stop the motor. Use this if you think that the stepper motor is moving further than you intended or if the stepper motor starts making noise that could indicate that it is having trouble moving. If you suspect the latter case, contact your tutor immediately.

11. The “DOWNLOAD DATA” button will download the data stored in the database directly to the tablet in a .csv file. You can then email the data to yourself or save it to a flash drive or SD card for later analysis.

12. The “CLEAR TEMP DATA” button will delete the temperature data stored in the database. It is recommended to do this in between each data collection for the same reasons specified under the “CLEAR DATA” button. There is a separate plot to visualize the temperature data as a function of time.

3.6.3 Controlling the Power Supply using the GUI

It is possible to control the DC power supply using the GUI. The DC power supply controls the supply current to the oven using channel 1 (Ch. 1) and to the solenoid coils using channel 2 (Ch. 2). As shown in Fig. 17 and Fig. 18, there are various entry fields, buttons, and display fields for conrolling and monitoring the state of the power supply. We will explain them here.

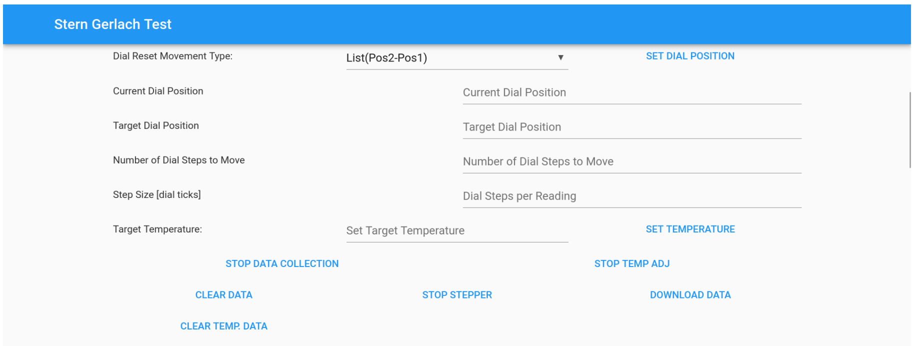

Figure 16: A screenshot of the GUI used to monitor and control the setup. The controls for rotating the dial controlling the position of the tungsten detector wire are shown as well as some of the other temperature and data collection related options.

1. The "Channel to set" row has a dropdown to select the channel that you wish to modify, e.g. channel 1 or 2. Underneath this are two entry fields. The left entry takes the value for the voltage in Volts that you would like to set. The entry on the right takes the value for the current in Amps that you would like to set.

2. The "Set Voltage" button, when pressed, will set the voltage of the channel selected in the dropdown to the voltage specified in the Voltage entry field.

3. The "Set Current" button, when pressed, will set the current of the channel selected in the dropdown to the current specified in the Current entry field.

4. The "READ POWER SUPPLY VALUES" button, when pressed will read the values currently set on the power supply for both channels 1 and 2 as well as the master control state and display them in the display fields below.

5. The "TURN CH. 1 ON" button will turn the output of channel 1 on. The text of this button will then change to "TURN CH. 1 OFF" and then will turn the Ch. 1 output off when pressed. Note, the master output and the channel 1 output both need to be turned on in order for current to flow through the circuit controlled by channel 1.

6. The "TURN CH. 2 ON" button will turn the output of channel 2 on. The text of this button will then change to "TURN CH. 2 OFF" and then will turn the Ch. 2 output off when pressed. Note, the master output and the channel 2 output both need to be turned on in order for current to flow through the circuit controlled by channel 2.

7. The "TURN MASTER OUTPUT ON" button will turn the master output on. The text of this button will then change to "TURN MASTER OUTPUT OFF" and then will turn the master output off when pressed. Note that if the master output is off no current will flow if any of the other channels are turned on.

8. The "Channel Powered:" header contains the on/off display status of each channel and the master output after having pressed the "READ POWER SUPPLY VALUES" button. There is a display field next to each "Ch. 1 Out:", "Ch. 2 Out: ", and "Master Out:" fields that will display "ON"/"OFF" depending on the state of the power supply at the time of the read operation.

9. The "Channel 1" header contains the status of the individual current and voltage states (values) for channel 1. In the "Voltage (Supply)" row there is a display field that will display the voltage value for channel 1 read during the read operation when the "READ POWER SUPPLY VALUES" button is pressed. The last field in the row displays the value in unit '[V]'. The same is true for the "Current (Supply)" row except that it displays the value for the current in '[A]' during the read operations when the "READ POWER SUPPLY VALUES" button is pressed.

10. The “Channel 2” header is similar to that of the “Channel 1” header except it reads the values for channel 2 and displays them.

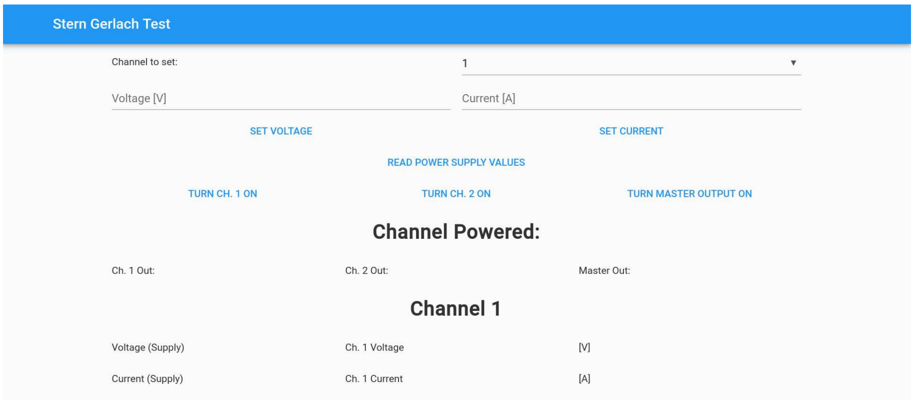

Figure 17: A screenshot of the GUI used to monitor and control the setup. The controls and readout for the power supply are shown.

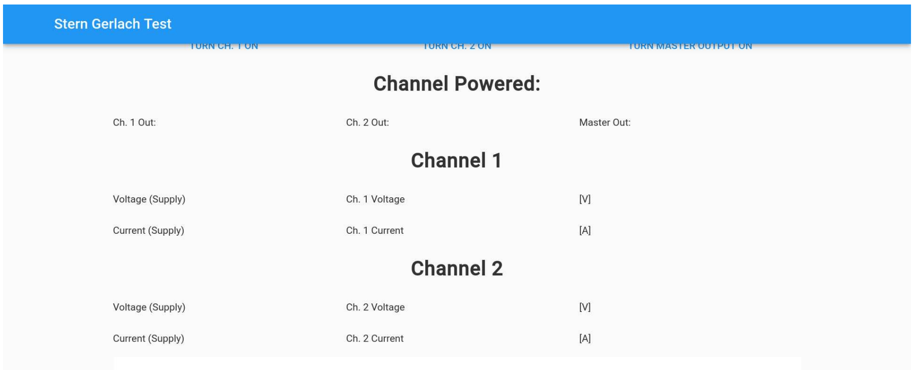

Figure 18: A screenshot of the GUI used to monitor and control the setup. The controls and readout for the power supply are shown.

3.6.4 Data Troubleshooting Plots in the GUI

To help with debugging a couple courtesy plots have been added to the GUI. The first courstesy plot shown, Fig. 19, presents a sample out put that one might expect to get with no applied magnetic field. The plot axes are taken as the subtick position during the run along the horizontal and the signal output current along the horizontal in mA. The plot updates regularly throughout the data collection process, however there is some delay (can be up to 30 s depending on the internet connection). The GUI collects the data stored in the database and plots it. Shown in this figure, for illustrative purposes, is why one should clear the data in between each run. The plot is not intended for final use, but to get a quick, “real-time” idea if the data being collected makes sense so that if there is a problem, the data collection can be stopped and some troubleshooting performed before trying again.
The second courtesy plot provided by the GUI is a temperature plot. This plot shows the temperature of the oven (in degrees C) as a function of time. This will allow to understand if the temperature is staying approximately constant over time or, in the case of a changing temperature, give an idea of how much the oven current should be changed to compensate.

3.7 Procedure for using the GUI

The students will primarily interact with the setup using the website-based GUI through a browser on the tablet(s) provided by the tutor. This can be slightly complicated initially. As such the general procedure

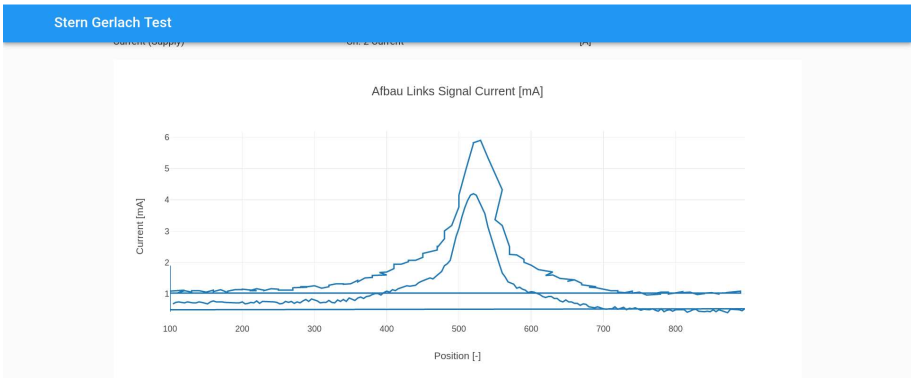

Figure 19: A screenshot of the signal current vs. detector position courtesy plot. This plot can assist in debugging and understanding the quality of data in case of problems.

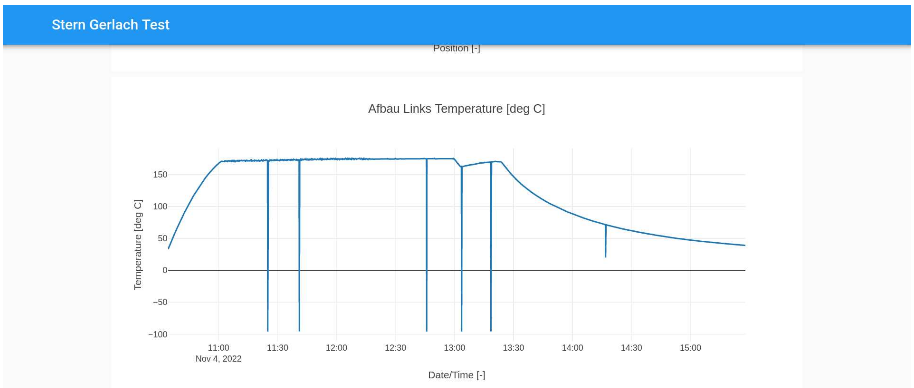

Figure 20: A screenshot of the oven temperature vs. time courtesy plot. This plot can assist in debugging temperature related issues during data taking.

for taking a sample data collection run will be outlined here.

1. If not already powered on, turn the tablet on by holding the power button for 3-5 seconds.
2. There should not be any login required.
3. The website for the GUI should be stored in the browser "favorites" section or otherwise bookmarked. If you have difficulty finding this ask your tutor.
4. Once the GUI has loaded, follow the general procedure for running the experiment.
5. Set the dial to the specified value using the Stepper motor controls specified in the previous section. We recommend setting the dial position using the "Number of Steps" setting in the dropdown menu.
6. After the dial is set, the temperature can be changed, if needed by setting the oven current on channel 1 following the specification outlined earlier in the manual and using the "Controlling the Power Supply using the GUI" section.
7. It is recommended to perform a read operation on the power supply using the "READ POWER SUPPLY VALUES" button each time prior to changing any power supply values.
8. Once the oven has reached a stable temperature, if necessary change the solenoid coil supply current using channel 2 of the power supply using the "Controlling the Power Supply using the GUI" section.
9. Set the "Current Dial Position", "Target Dial Position", and "Number of Dial Steps to Move" fields as needed and press the "START DATA COLLECTION" button.

10. You should notice the stepper motor rotating the dial with some delay. The delay is to allow the signal current to stabilize.

11. Monitor the data and read from the setup.

12. If you notice problems you can stop data collection and trouble shoot and try again. If problems persist contact the tutor.

13. Once the data collection has stopped, download the data to the tablet via the “DOWNLOAD DATA” button and store the data for later use by sending to yourself via email or using a flash drive.

14. Setup for the next data collection.

Of course, this procedure is general and sometimes only a subset of the above procedure will be implemented. If you have questions, you can always contact the tutor.

4 Important Notes

Before the start of lab-course, potassium is refilled in oven. So you should have enough potassium to do the experiment. But if you think that potassium is exhausted (i.e. you do not see a peak and only measure noise), contact the tutor.
The amplifier output is in units of current (mA).
The higher the temperature that the oven is operated at, the more potassium is used. Please do not increase the temperature unneccesarily. Potassium is expensive. Do not go above 175 degrees.
For both setups, the detector current is roughly between 4.1 A and 4.3 A. The current needs to stabilize when you are taking a measurement. the current naturally decreases (slowly) when you set it to a certain value, because of the detector wire resistance changing with temperature. If the current decreases below 4.1 A then you might need to increase it a little bit, in order to keep the dark current at acceptable levels. If you increase the current then you would need to wait for some time so that the current can stabilize. Never increase the current beyond 4.3 A.
For the coil current, you may vary this from 0 to 2 A. Do not go beyond 2 A.
If there are any questions, please contact the tutor. This is a sensitive apparatus, and any wrong setting of voltage / current / temperature can harm the apparatus. So, please be careful.

5 Analysis

The aim of the evaluation is to review the two previously mentioned theories. Therefore, proceed as follows:

- Plot the current values that you recorded during the heating of the furnace versus the temperature. Defend why the temperature used was the temperature at which the experiment should reasonably be carried out.

- For various coil currents, plot the detector current ($\sim$ particle current density) versus the displacement of the detector.

- Determine the magnetic moment μ_B
  - using the theory of an arbitrarily narrow beam box (by plotting $u_0^{(0)}$ versus $\frac{b}{3}$, cf. equation 15)
  - using equation (18) for a real beam box (by plotting $u_0^{(0)} - \frac{C}{3u_0^{(0)}}$ versus $\frac{b}{3}$ - therefore, the real beam profile has to be parametrized as shown in Figure 4).

- Therefore, the positions $u_0^{(0)}$ of both maxima have to be determined for different field inhomogeneities.
- The conversion of the coil current into the field inhomogeneities can be found in Appendix B.1. Do not forget to write down which setup you have used!!!
- Discuss the differences in your results and comment on how reasonable the usage of the real-beam profile is. Discuss all other items that can influence on your measurement.

A Mathematical background

A.1 Two-wire field

The magnetic induction of two anti-parallel electrical currents at the distance $2a$ is obtained by adding up their individual components

$$\vec{B_i} = \frac{\vec{I_i} \times \vec{r_i}}{2\pi \cdot r_i^2}.$$

Knowing $\vec{I_1} = -\vec{I_2} = \vec{I}$, one has

$$B(\vec{r}) = \frac{\mu_0 I a}{\pi r_1 r_2}.$$

In order to let the atomic beam undergo a substantially constant force, it has to traverse the magnetic analyser at a point with almost constant field inhomogeneity. Therefore, it has to be determined at which distance from the wires (plane of wires $z = -z_0$) the field inhomogeneity is as constant as possible, i.e. $\frac{\partial B}{\partial z} = const$. This plane is chosen to be at $z = 0$.

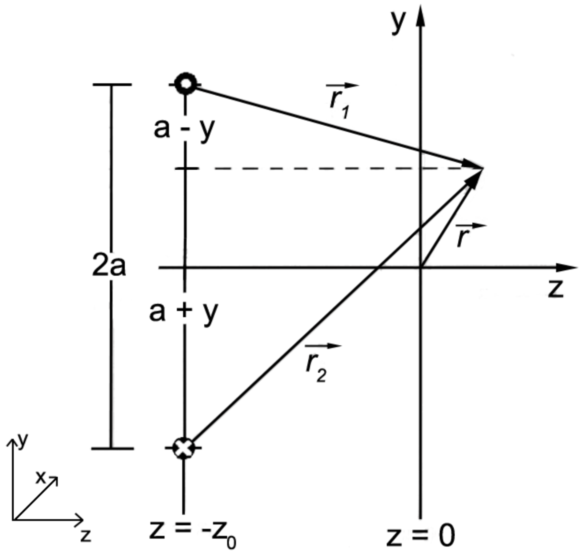

Figure 21: Definition of a coordinate system

The following relationships for the distances r_1 and r_2 can be extracted from figure 21:

$$r_1^2 = (a-y)^2 + (z+z_0)^2$$
$$r_2^2 = (a+y)^2 + (z+z_0)^2$$

By inserting into the equation above, this results in

$$B(y,z) = \frac{\mu_0 \cdot I \cdot a}{\pi} \cdot \left[\left(a^2 - y^2\right)^2 + 2\left(z+z_0\right)^2\left(a^2+y^2\right) + \left(z+z_0\right)^4\right]^{-\frac{1}{2}} \tag{19}$$

and by taking the derivative of this with respect to z the field inhomogeneity is obtained to

$$\frac{\partial B}{\partial z} = -\frac{2 \cdot \mu_0 \cdot I \cdot a \cdot (z+z_0)}{\pi} \cdot \frac{a^2 + y^2 + (z+z_0)^2}{\left[\left(a^2 - y^2\right)^2 + 2\left(z+z_0\right)^2\left(a^2+y^2\right) + \left(z+z_0\right)^4\right]^{\frac{3}{2}}}.$$

At $z = 0$, the inhomogeneity dependence on y should disappear. To find this plane, $\frac{\partial B}{\partial z}$ is expanded up to first order in y^2 at $y = 0$. The approximation yields

$$\frac{\partial B}{\partial z}(y,z) \approx -\frac{2\mu_0 I \cdot a \cdot (z+z_0)}{\pi\left(a^2 + (z+z_0)^2\right)^2} \cdot \left[1 + 2y^2 \cdot \frac{2a^2 - (z+z_0)^2}{\left(a^2 + (z+z_0)^2\right)}\right].$$

Thus, the dependence of y vanishes for $z_0 = \sqrt{2}a$. This is the distance of the atom beam from the fictitious wires.
For the calculation of the magnetic moment, it is important to know the field inhomogeneity. It can not be measured directly. However, it can be calculated from the magnetic field strength under the assumption of a linear relationship between B and $\frac{\partial B}{\partial z}$ for small deflections z. Now, the proportionality factor $\epsilon = \left|\frac{\partial B}{\partial z}\right| \cdot \frac{a}{B}$ should be determined in the area around $y = 0$. Therefore, $\epsilon(y, z)$ is expanded up to first order in y^2 at $y = 0$ like above:

$$\epsilon\,(y,z) \approx \frac{2a\,(z+z_0)}{a^2+(z+z_0)^2} \cdot \left(1 + \frac{3a^2-(z+z_0)^2}{\left(a^2+(z+z_0)^2\right)^2} \cdot y^2\right).$$

The system of cover plates of the apparatus is designed in a way that the atomic beam has a width of approximately $\frac{4}{3}a$ in y-direction. In the area of this beam box $\epsilon(y, 0)$ changes slightly with y, therefore the average of the highest possible value epsilon $\epsilon\left(\frac{2}{3}a, 0\right) \approx 0.9894$ and the lowest value $\epsilon(0, 0) \approx 0.9428$ is used to calculate the inhomogeneity. Thus, the conversion factor is $\epsilon \approx 0.9661$.

A.2 Real beam cross-section, method B

A.2.1 Beam cross-section

Now let us discuss the model for the real beam cross section, described in section 2.6. Looking at the equations (17), we see that $I_0(z)$ is defined as two-times-differentiable. Based on this, the determination of the particle current density $I(u)$ depends on the inhomogeneity of the magnetic field, i.e. of b (equation (10)). The maxima of $I(u)$ are located at the positions $u_0(b)$, which now more or less differ from the positions $u_0^0 = \pm\frac{b}{3}$, i.e. from the approximation for an infinitesimal beam box. To determine the function $u_0(b)$, we assume

$$\frac{\mathrm{d}I}{\mathrm{d}u}(u_0) = 0.$$

The derivative with respect to u can now be taken into the integral, as can be seen in the following calculation

$$\begin{aligned}\frac{\mathrm{d}I}{\mathrm{d}u} &= \frac{\mathrm{d}}{\mathrm{d}u} a \int_{-D}^{+D} I_0(z) \frac{e^{-\frac{b}{|u-z|}}}{|u-z|^3}\mathrm{d}z \\ &= a \int_{-D}^{+D} I_0(z) \frac{\partial}{\partial u} \frac{e^{-\frac{b}{|u-z|}}}{|u-z|^3}\mathrm{d}z.\end{aligned}$$

As one can easily verify, the replacement of $\frac{\partial}{\partial u}$ with $-\frac{\partial}{\partial z}$ leaves the integrand unchanged:

$$\frac{\mathrm{d}I}{\mathrm{d}u} = -a \int_{-D}^{+D} I_0(z) \frac{\partial}{\partial z} \frac{e^{-\frac{b}{|u-z|}}}{|u-z|^3}\mathrm{d}z.$$

By partial integration[1], it is now possible to move the differentiation to I_0. Please check that here the first term from the partial integration vanishes.

$$\frac{\mathrm{d}I}{\mathrm{d}u} = a \int_{-D}^{+D} \frac{\mathrm{d}I_0(z)}{\mathrm{d}z} \frac{e^{-\frac{b}{|u-z|}}}{|u-z|^3}\mathrm{d}z.$$

Inserting equation (17) returns

$$\frac{\mathrm{d}I}{\mathrm{d}u} = a i_0 \left\{ \int_{+D}^{-p} - \int_{-p}^{+p} \frac{z}{p} - \int_{+p}^{+D} \right\} \frac{e^{-\frac{b}{|u-z|}}}{|u-z|^3}\mathrm{d}z.$$

[1]Reminder: $\int_a^b f(x) \cdot g'(x)\mathrm{d}x = \left(f(x) \cdot g(x)\right)\big|_a^b - \int_a^b f'(x) \cdot g(x)\mathrm{d}x$

Both occurring integrals can be solved analytically (e.g. with Maple) and result in

$$\frac{\mathrm{d}I}{\mathrm{d}u} = \frac{ai_0}{pb^2} \cdot F(u)$$

with the solution function

$$F(u) = -|u+p|e^{-\frac{b}{|u+p|}} + |u-p|e^{-\frac{b}{|u-p|}} + p\frac{b+|u+D|}{u+D}e^{-\frac{b}{|u+D|}} + p\frac{b+|u-D|}{u-D}e^{-\frac{b}{|u-D|}}.$$

It immediately yields the equation for determining the positions of the maxima

$$F(u_0) = 0.$$

One can see now that $F(u_0)$ is point-symmetrical. The solution function $u_0(b)$, which indicates the position of the maxima, is thus mirror symmetric. By this simplification, we can restrict to the determination of the positive values only.

A.2.2 Asymptotic behaviour for large fields

If the field inhomogeneity is sufficiently large, u_0 converges the solution which is given by the infinitesimally narrow beam box.
If we now assume

$$\frac{u_0}{p}, \frac{u_0}{D}, \frac{b}{p}, \frac{b}{D} \gg 1, \tag{20}$$

then the following calculations describes a more precise behaviour of the function $u_0(b)$ for large fields. With the help of the aforementioned approximation, $F(u)$ can be developed as a Taylor series, for which we need the following function:

$$f(u) = u \cdot e^{-\frac{b}{u}}. \tag{21}$$

The relevant derivatives are

$$\begin{aligned} f^{(3)}(u) &= \tfrac{b^2}{u^4}\left(\tfrac{b}{u} - 3\right)e^{-\frac{b}{u}} \\ f^{(5)}(u) &= 12\tfrac{b^2}{u^6}\left(5\left(\tfrac{b}{u} - 1\right) + \tfrac{1}{12}\tfrac{b^2}{u^2}\left(\tfrac{b}{u} - 15\right)\right)b^{-\frac{b}{u}}. \end{aligned}$$

Up to the sixth derivation, only the third and fifth derivative are of interest, because only in this case the coefficients do not vanish.
Thus, abortion after the sixth element results in:

$$F(u) = p\left(D^2 - \frac{1}{3}p^2\right) \cdot f^{(3)}(u) + \frac{p}{12}\left(D^4 - \frac{1}{5}p^4\right) \cdot f^{(5)}(u) + \dots. \tag{22}$$

From this we obtain, once more by setting equation (22) to 0, the equation for u_0

$$0 = \left(D^2 - \frac{1}{3}p^2\right)\left(\frac{b}{u_0} - 3\right) + \frac{D^4 - \frac{1}{5}p^4}{u_0^2}\left(5\left(\frac{b}{u_0} - 1\right) + \frac{1}{12}\frac{b^2}{u_0^2}\left(\frac{b}{u_0} - 15\right)\right). \tag{23}$$

The further way to determine u_0 is explained in the theory section (section 2.6.2).

B Figures

B.1 Calibration curves

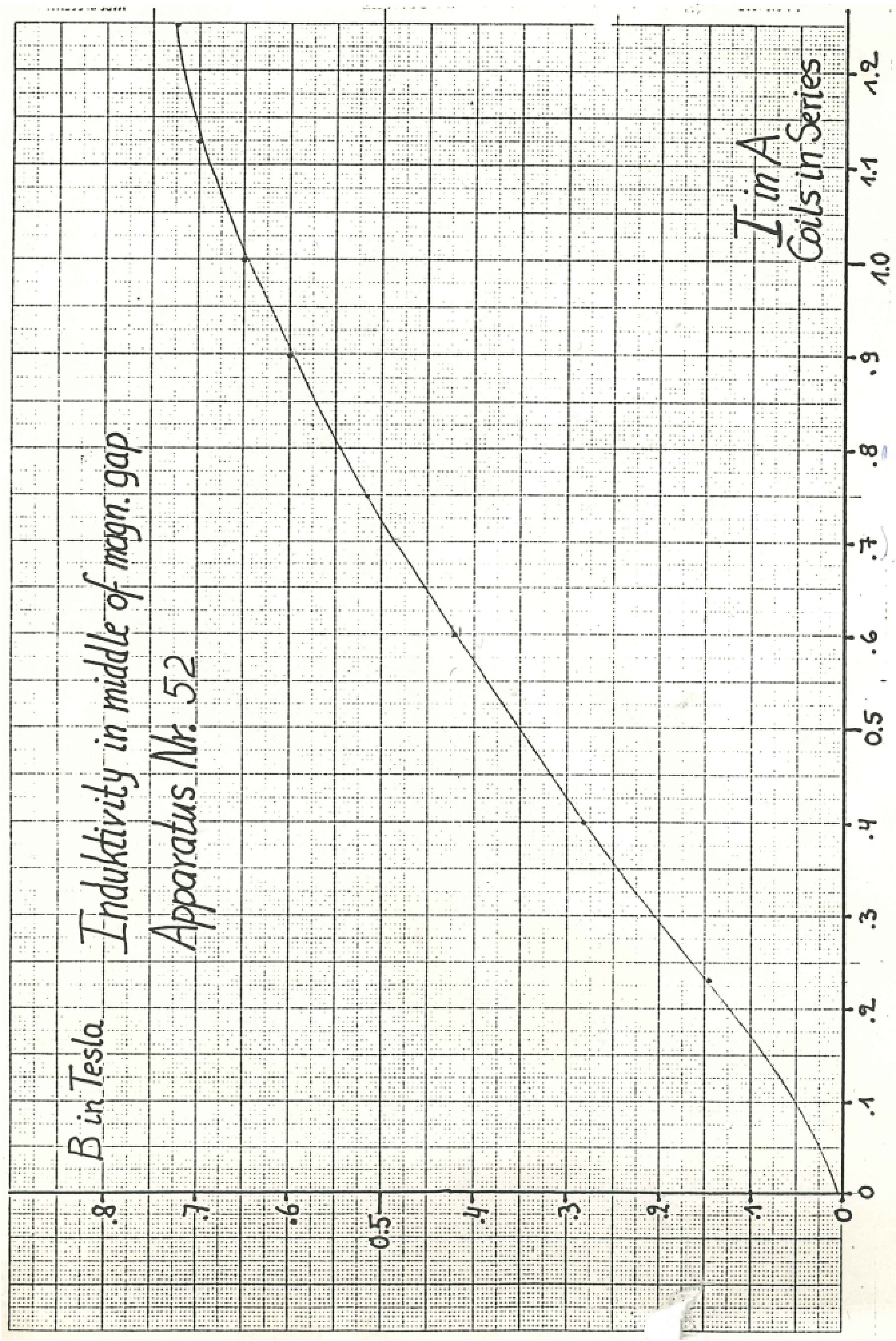

Figure 22: Calibration curve of the magnet No. 52 (set-up A)

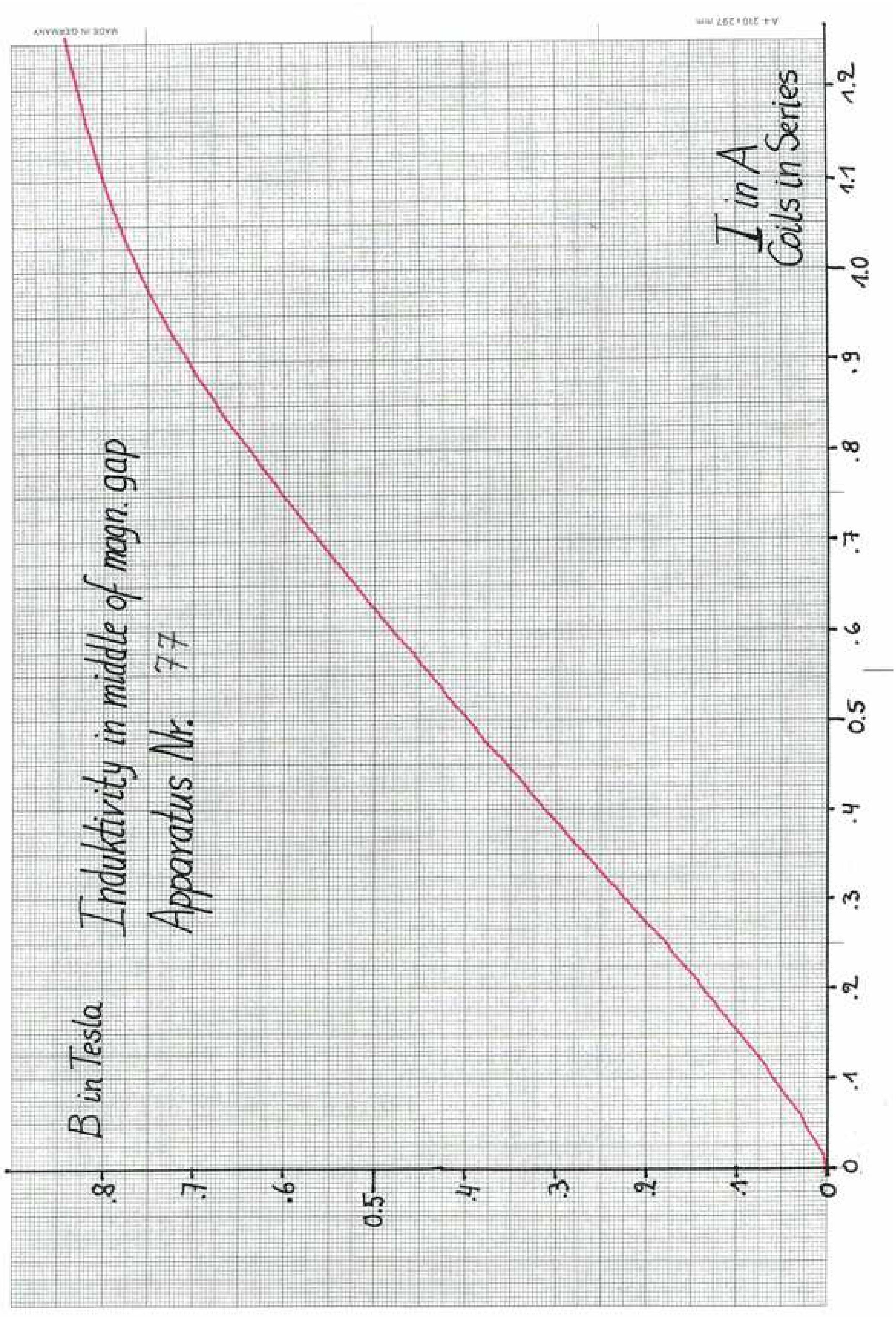

Figure 23: Calibration curve of the magnet No. 77 (set-up B)